Opto-Electronic Advances

Original Article

2022, Vol. 5, No. 11

DOI: 10.29026/oea.2022.200066

Exciton-polariton based WS_2 polarization modulator controlled by optical Stark beam

Mahnoor Shahzadi[1], Chuyuan Zheng[1], Sheraz Ahmad[2], Shanshan Wang[1] and Weili Zhang[1]*

The recent era of fast optical manipulation and optical devices owe a lot to exciton-polaritons being lighter in mass, faster in speed and stronger in nonlinearity due to hybrid light-matter characteristics. The room temperature existence of polaritons in two dimensional materials opens up new avenues to the design and analysis of all optical devices and has gained the researchers attention. Here, spin-selective optical Stark effect is introduced to form a waveguide effect in uniform community of polaritons, and is used to realize polarization modulation of polaritons. The proposed device basically takes advantage of the spin-sensitive properties of optical Stark effect of polaritons inside the WS_2 microcavity so as to guide different modes and modulate polarization of polaritons. It is shown that polaritonic wavepacket of different mode profiles can be generated by changing intensity of the optical Stark beam and the polarization of polaritons can be controlled and changed periodically along the formed waveguide by introduction birefringence that is sensitive to polarization degree of the optical Stark beam.

Keywords: Stark beam; polaritons; modulator; TMDs; polarization degree

Shahzadi M, Zheng CY, Ahmad S, Wang SS, Zhang WL. Exciton-polariton based WS_2 polarization modulator controlled by optical Stark beam. *Opto-Electron Adv* **5**, 200066 (2022).

Introduction

In the quite striking development of optoelectronic industry, a prominent role is played by exciton-polaritons. They are low mass and high-speed quasi particles which are generated due to the strong light-matter coupling[1–5]. The strong nonlinearity and room temperature existence of polaritons have given the open ways to deploy them in applications of optical information and optoelectronic devices[4–9]. Transition metal chalcogenides (TMDs) also have been focused for electric controllability as well[10]. Usually, microcavities with high quality factor play a vital role for the strong exciton-photon coupling thus enhancing stability of polaritons at room temperature[11–13]. Optical Stark (OS) effect is optoelectronic interaction arising from the hybridization of photonic and electronic states[4,7,10,17,25]. Spin-selective OS excitation, with the additional spin degree of freedom, offers new prospects to realize spin logic and spin-Floquet topological phases for ultrafast optical implementations and quantum information applications[14–18]. Apart from the fundamental criterion of strong light-matter coupling, polaritonic applications using OS effect also enforces material selection requirement, like high-charge mobility for electronic integration and room-temperature operation for practical applications[19]. Recently, TMDs such as WS_2, WSe_2, MoS_2 and $MoSe_2$ are quite tempting for researchers due to their attractive features such as

[1]School of Information and Communication Engineering, University of Electronic Science and Technology of China, Chengdu 611731, China; [2]College of Petroleum Engineering, China University of Petroleum, Beijing 102249, China.

*Correspondence: WL Zhang, E-mail: wl_zhang@uestc.edu.cn

Received: 11 October 2020; Accepted: 2 April 2021; Published online: 31 March 2022

direct energy band gapes, high charge carrier mobility, strong light matter coupling and promoting polaritons at room temperature[20–22]. It has been reported that a large OS shift of 21 meV is realizable in WS_2 excitons[11], paving a way for various applications based on OS shift in TMDs in particular WS_2 microcavity. Various characteristics of the polaritons in WS_2 microcavity, has been studied and manipulated in different ways for design of optoelectronic devices[6,10,11,21,26]. For example, surface Plasmon polariton graphene Photodetectors have been reported in which they couple graphene with a plasmonic grating and exploit the resulting surface plasmon polaritons to deliver the collected photons to the junction region of a photodetector with 400% enhancement of responsivity and a 1000% increase in photoactive length[6]. Further, tuneable exciton-polaritons have been observed in hybrid monolayer WS_2-plasmonics structure aimed for nano-antenna system[18]. Currently, polariton based LED in monolayer of WS_2 is designed which is stable at room temperature and have quantum efficiency of 0.1%[23]. Recently we have proposed an all optical polariton based multimode interferometer, in which OS shift is used as a controlling parameter to control modal interference of polaritons without the consideration of polarization issue[26]. While exploiting spin characteriscs of polaritonic devices are still far from enough and deserves further study. As we have discussed above the tempting applications of WS_2 material, here a polarization modulator of polaritons is proposed to be realized in a WS_2 microcavity taking advantage of spin selective characteristics of OS effect i.e. energy of the excitonic fraction of polaritons inside the WS_2 microcavity can/can't be shifted by co-polarized/cross-polarized OS beam. This effect is used to guide wavepacket of polaritons with controlled birefringence and thus modulate their polarization along the transmission path. The polarization state of polaritons can also be tuned by changing the energy (i.e., change the energy shift of polaritons) and effective area of the OS beam (i.e., change transmission length of polaritons) and thus, an all optical controllable polarization modulator is proposed.

Principle of operation

Here we describe the principle of operation to realize our proposed idea. In Fig. 1 below, the microcavity consists a WS_2 monolayer (i.e., the active layer) sandwiched by two distributed Bragg reflectors (DBRs). We suppose the center wavelength of the DBRs is the same as the excitonic resonance wavelength $\lambda_0 = 601$ nm. Based on this structure, cavity photons and excitons can couple strongly and generate the polaritons just like the way previously reported in ref.[29]. A circularly polarized OS beam acts as a writing beam that radiates on WS_2 cavity and generates a potential in the uniform cavity, providing a waveguide of polaritons in the WS_2 layer. In order to practically realize our proposed idea here, we use the OS beam, which can be a strong laser pulse red-detuned from the excitonic energy so as to induce an almost instantaneous and rigid shift of the lower and upper polariton branches. Here we demonstrate that through this shift, a continuous wave that can instantaneously cause a shift in the energy of excitons and create a potential (up to few meV to few tens of meV) of polaritons, the so-called OS effect. This OS effect causes the shift in the polariton quantum states and can be used to manipulate in various ways for optoelectronic applications[1,3,7,22,26]. Here, a polaritonic potential, i.e., OS shift, is created just like in ref.[11] and used in an innovative way to form a waveguide channel of polaritons along the x-direction with a width of 10 μm (i.e., in the y-direction). As shown in Fig. 1, the region with generated potential (core region) has an effective refractive index larger than other regions (cladding region). Taking advantage of the spin selectively characteristics of the OS effect, the birefringence of the waveguide can be controlled easily via controlling polarization and intensity of the OS beam. Thus, the waveguide channel can be used to transmit different modes of polariton wavepacket with polarization sensitivity, to control their interference, and finally to modulate their degree of polarization. In our case, we use the G-P model to describe the propagation of polaritons[7,27,28]. Our analysis mainly focuses on the polarization of polaritons, so we use this model with some presupposes. First, the excitonic energy equals the energy of the cavity photon. As the energy of the cavity photon is fixed, the complex refractive index of the WS_2 is taken as a constant value. Based on this, the effective mass and decay rate (depend on the loss of the cavity and the imaginary parts of the refractive index of WS_2) of polaritons can be determined. Second, the pump/gain of the polaritons is assumed to balance with the decay rate of the polaritons, thus both the pump term and the decay term did not appear in the model. Third, the microcavity is assumed to work below the nonlinear threshold, and the nonlinear scattering term is neglected in the model. The imaginary parts of the refractive index and anisotropic characteristics[30–32] would be left for our future work.

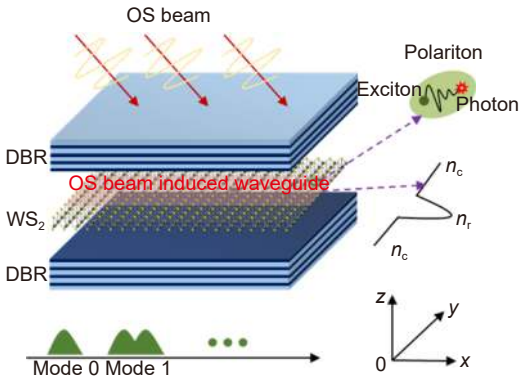

Fig. 1 | Structure of proposed model. The optical Stark beam is added to the cavity and a waveguide generated. The directions used in this paper are set by the coordinate.

Quantum description of spin selective OS effect

The optical pumping will raise or lower the magnetic quantum number of excitons by one, and a circularly polarized Stark beam will prepare the spin-polarized excitons with blue-shifted excitonic energy[11,25,26,32]. As indicated in Fig. 2, the equilibrium state of excitons (solid red and purple lines) will be shifted to a new state (dashed red and purple lines) when the OS beam is added, and the energy gap (excitonic energy) is increased by $\Delta E_x^{\sigma^\pm}$. The exciton state of $|-1/2\rangle$ at the conduction band and $|+1/2\rangle$ at the valence band can couple with right circularly polarized (σ^-) cavity photons, while the exciton state of $|+1/2\rangle$ at the conduction band and $|-1/2\rangle$ at the valence band can couple with left (σ^+) circularly polarized cavity photons. Under the strong coupling condition, i.e., the exciton-photon coupling rate parameterized by the Rabi splinting energy $\hbar\Omega/2$ is much larger than their decay rate, so polaritons are formed (see the upper and lower polariton branches "$E_{\mathrm{tPLP}}^{\sigma^\pm}$"). Thus, the OS effect of polaritons will inherit the spin selective characteristics of their excitonic part e.g., OS beam will blue shift the polaritons with polarization sensitivity.

Effective refractive index method of polariton wavepacket

This energy shift can be described as

$$\Delta E_x^{\sigma^\pm} \propto \frac{\boldsymbol{M}_{\mathrm{ab}}^{\pm}|E_{\mathrm{os}}|^2}{2\Delta}\,. \tag{1}$$

From Eq. (1), we can see that energy shift of excitons is related to the OS beam intensity "$|E_{\mathrm{os}}|^2$" and the energy difference "Δ" between the OS photons and excitons. In Eq. (1) $\boldsymbol{M}_{\mathrm{ab}}^{\sigma^\pm} = \begin{bmatrix} 1 & 0 \\ 0 & 1 \end{bmatrix}\begin{bmatrix} +\sigma \\ -\sigma \end{bmatrix}$ is a polarization matrix, and it accounts for the spin selective characteristics of the OS effect. The excitonic shift influences the dispersion curves of the polaritons, which can be calculated from the Floquet quasi-states theory and reads[7,21,25,33]. The optical Stark beam causes energy shift of excitons just like adding an external electronic field. To realize this, the photon energy of the Stark beam should be

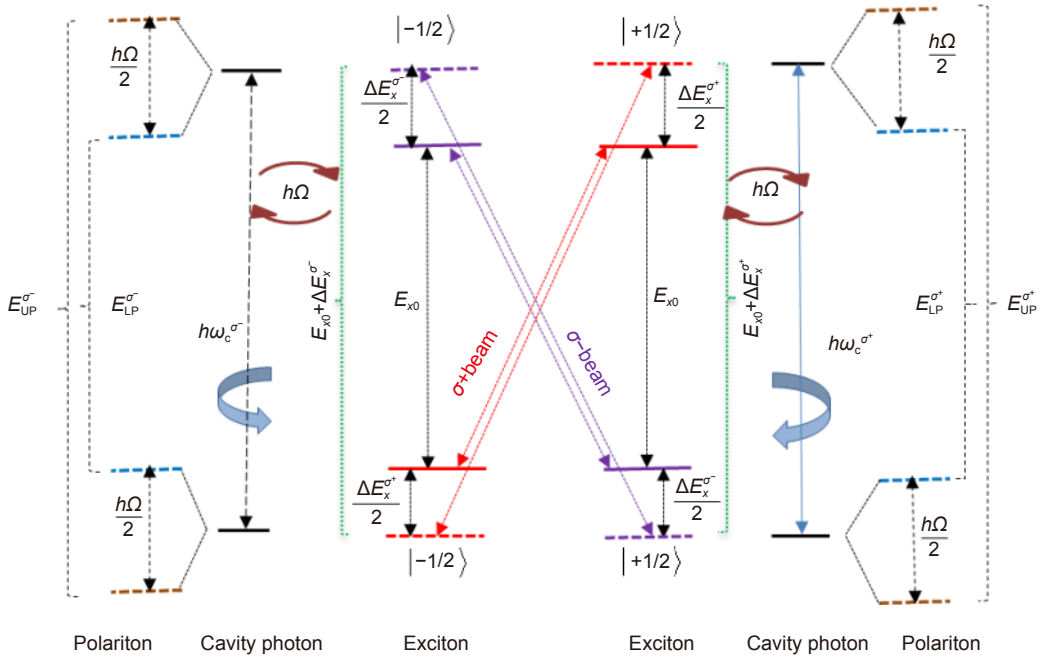

Fig. 2 | Two level excitonic states and their strong coupling with cavity photons when the OS beam is added.

smaller than the exciton energy; that is optical Stark beam does not increase the population of excitons. The energy shift of exciton can be calculated as given in Eq. (1).

$$E_i^{\sigma^\pm} = \frac{1}{2}\left(E_c^{\sigma^\pm}(k) + E_x^{\sigma^\pm} + \frac{\Delta E_x^{\sigma^\pm}}{2} + (-1)^i\sqrt{\left(E_c^{\sigma^\pm}(k) + E_x^{\sigma^\pm} + \frac{\Delta E_x^{\sigma^\pm}}{2}\right)^2 + \Omega_R{}^2}\right). \tag{2}$$

Equation (2) reflects the spin sensitive case, wherein "$\sigma^\pm$" correspond to the left and right circularly polarizations, $i = 1$ or $i = 2$ depicts the lower or upper polariton branches respectively, $E_c^{\sigma^\pm}(k) = E_{c0}^{\sigma^\pm} + \frac{\hbar k_{||}{}^2}{2m_c}$ and $E_x^{\sigma^\pm} = E_{x0}^{\sigma^\pm} + \frac{\hbar k_{||}{}^2}{2m_e}$ are the photonic and excitonic energies respectively (where $k_{||}$ is the in-plane wave vector, $E_{c0}^{\pm}/E_{x0}^{\pm}$ is the energy of cavity photons/excitons for $k_{||} = 0$ and m_c/m_e is the mass of cavity photons/excitons). The OS shift $\Delta E_x^{\sigma^\pm}$ is directly proportional to the intensity of the OS beam and inversely proportional to the energy difference between the excitons and the OS photons. We can calculate the effective refractive index as

$$\begin{aligned} k_{||}n_r^{\sigma^\pm} &= \frac{1}{\hbar}\sqrt{2m_p\left(E_i^{\sigma^\pm}(k_{||}, \Delta E_{os}^{\sigma^\pm} \neq 0) - E_i^{\sigma^\pm}(k_{||}{=}0, \Delta E_{os}^{\sigma^\pm} \neq 0)\right)} \\ k_{||}n_c^{\sigma^\pm} &= \frac{1}{\hbar}\sqrt{2m_p\left(E_i^{\sigma^\pm}(k_{||}, \Delta E_{os}^{\sigma^\pm}{=}0) - E_i^{\pm}(k_{||}{=}0, \Delta E_{os}^{\pm}{=}0)\right)}, \end{aligned} \tag{3}$$

where m_p stands for the effective mass of the polaritons, and its value is calculated as $m_p = \frac{m_e}{|X|^2} + \frac{m_c}{|C|^2}$ ($|X|^2/|C|^2$ is the fraction of excitons/cavity photons, m_e/m_c is the effective mass of excitons/cavity photons)[27]. Using Eq. (2) polarization-dependent refractive index of the core ($n_r^{\sigma^\pm}$) and cladding ($n_c^{\sigma^\pm}$) region can be calculated. Finally, the guided mode of polaritons can be calculated from the guided-mode theory of a plane waveguide structure. The guided modes satisfy the wave matching condition $f(N_m^{\sigma^\pm}) = 0$, and the function f reads[28–32].

$$\begin{aligned} f(N_m^{\sigma^\pm}) = m\pi &+ \arctan\left(\frac{(n_r^{\sigma^\pm})^{2\alpha}}{(n_c^{\sigma^\pm})^{2\alpha}}\sqrt{\frac{(N_m^{\sigma^\pm})^2 - n_c^2}{(n_r^{\sigma^\pm})^2 - (N_m^{\sigma^\pm})^2}}\right) \\ &+ \arctan\left(\frac{(n_r^{\sigma^\pm})^{2\alpha}}{(n_c^{\sigma^\pm})^{2\alpha}}\sqrt{\frac{(N_m^{\sigma^\pm})^2 - n_c^2}{(n_r^{\sigma^\pm})^2 - (N_m^{\sigma^\pm})^2}}\right) \\ &- k_{||}W\sqrt{(n_r^{\sigma^\pm})^2 - (N_m^{\sigma^\pm})^2}, \end{aligned} \tag{4}$$

where $\alpha = 0$ or $\alpha = 1$ describes TE or TM modes respectively, m is an integer number that corresponds to the order of mode, W is the width of the waveguide, and $N_m^{\sigma^\pm}$ is the effective refractive index of mode "m". Here we choose $\alpha = 0$ and study the TE modes as an example. The polaritonic waveguide generated by the OS beam will have encounter birefringence "$\Delta N_m = N_m^{\sigma^+} - N_m^{\sigma^-}$" when a change in polarization of the OS beam occurs. The profile of the polaritons along the waveguide can be written as a coherent superposition of individual modes.

$$\begin{aligned} \psi^{\sigma^\pm} &= \sum_{m=0,1,2\cdots}\psi_m^{\sigma^\pm} \\ &= \sum_{m=0,1,2\cdots}\cos\left(k_{||}\sqrt{(n_r^{\sigma^\pm})^2 - (N_m^{\sigma^\pm})^2}x\right)\exp\left(-ik_{||}N_m^{\sigma^\pm}y\right). \end{aligned} \tag{5}$$

Results and discussion

First, we take the OS beam in the left (σ^+) polarization direction as an example. Fig. 3 shows the effective refractive index as a function of the OS shift $\Delta E_x^{\sigma^+}$ for $k_{||} = 0.2\pi/\lambda_0$. It is clear from Fig. 3 that the OS shift-induced waveguide begins to support the fundamental mode (i.e., n_0) when $\Delta E_x^{\sigma^+} > 3.5$ meV and two modes (i.e., n_0 and n_1) are supported when $\Delta E_x^{\sigma^+} > 8$ meV. In the right (σ^-) polarization direction, the case is similar and not repeated here. Proceeding in this way and use Eq. (5) we have plotted Fig. 4 below, which describes the evolution of the polariton modes when σ^+ polarized Stark beam with $\Delta E_x^{\sigma^+} = 5$ meV is applied. In this case, the waveguide is formed only for σ^+ polarized mode, and the waveguide only supports the fundamental mode, as shown in Fig. 4(a). Along the length of waveguide intensity of σ^+ polarized polaritons remains constant as shown in Fig. 4(b).

When the OS shift increases, the waveguide supports more modes of polaritons. Figure 5(a) and 5(b) show the case when $\Delta E_x^{\sigma^+} = 22$ meV. It can be seen that two modes, i.e., mode 0 and mode 1, are supported in the σ^+

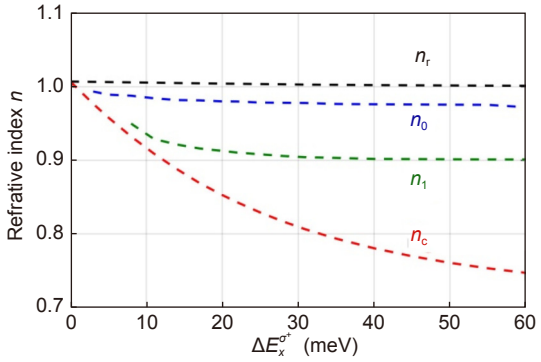

Fig. 3 | Effective refractive index versus OS shift "$\Delta E_x^{\sigma^+}$".

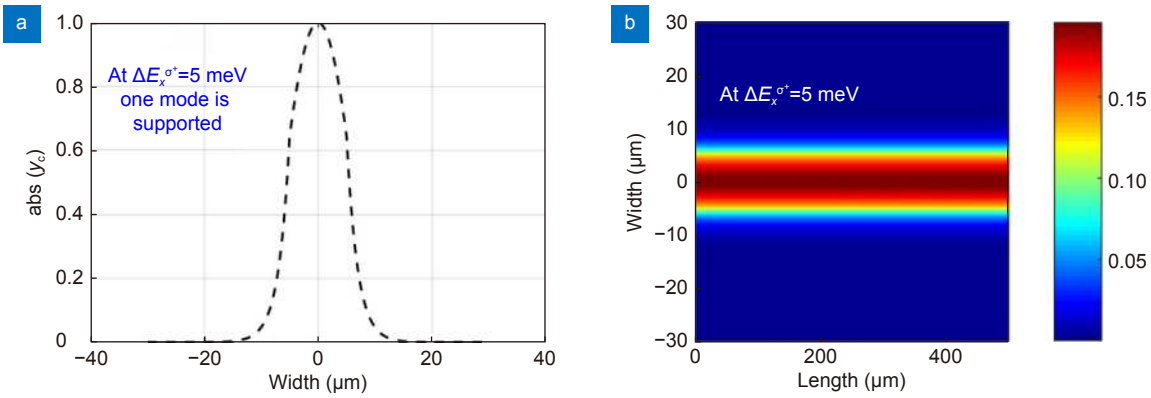

Fig. 4 | Mode profile of polariton wavepacket for polarized OS beam when $\Delta E_x^{\sigma^+}$ = 5 meV. (**a**) Only one mode is supported at $\Delta E_x^{\sigma^+}$= 5 meV. (**b**) A full map of the field distribution in the *x*-*y* plane at $\Delta E_x^{\sigma^+}$= 5 meV.

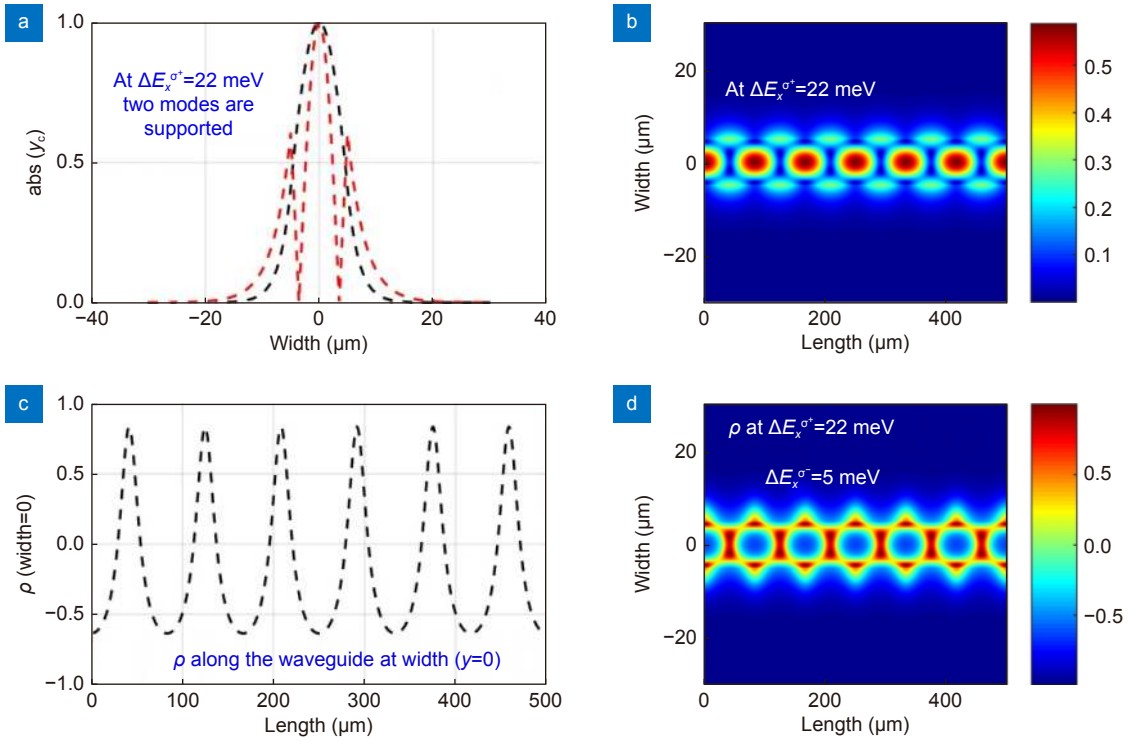

Fig. 5 | Mode profile and value of polarization degree *ρ*. (**a**) two modes are supported at $\Delta E_x^{\sigma^+} = 22$ meV and $\Delta E_x^{\sigma^-} = 0$ meV . (**b**) The full map of the field distribution in the *x*-*y* plane at $\Delta E_x^{\sigma^+} = 22$ meV and $\Delta E_x^{\sigma^-} = 0$ meV. (**c**) The modulation curves of *ρ* along the *x*-direction when *y* = 0 at $\Delta E_x^{\sigma^+} = 22$ meV and $\Delta E_x^{\sigma^-} = 5$ meV. (**d**) The full map of value *ρ* in the *x*-*y* plane at $\Delta E_x^{\sigma^+} = 22$ meV and $\Delta E_x^{\sigma^-} = 5$ meV.

polarized direction. When traveling along the waveguide, the two modes interfere with each other, and the total intensity of the polaritons varies periodically along the waveguide. Figure 5(c) and 5(d) show the case when OS beam is added to both σ^+ and σ^- polarized directions with different intensity, i.e., the shift are $\Delta E_x^{\sigma^+} = 22$ meV and $\Delta E_x^{\sigma^-} = 5$ meV. Thus, the waveguide support two modes in σ^+ polarization and one mode in σ^- polarization.

The corresponding value of polarization degree $\rho = \dfrac{\left(\left|\psi^{\sigma^+}\right|^2 - \left|\psi^{\sigma^-}\right|^2\right)}{\left(\left|\psi^{\sigma^+}\right|^2 + \left|\psi^{\sigma^-}\right|^2\right)}$ is given. Figure 5(c) shows the value of *ρ* along the waveguide (*x*-direction) for $y = 0$, wherein *ρ* varies periodically along the waveguide with peak and dip value of =0.45 and −0.9, respectively. For our work, the highest achievable peak/dip is 0.9/−0.9, while the lowest is 0.45/−0.45, respectively. The range of modulation speed depends on the response speed of polaritons, which is in the picosecond scale. The full map of *ρ* in the *x*-*y* plane is given in Fig. 5(d), which is reflecting the function of polarization modulation.

It is easy to understand that the modulation depth/range and period can be changed by changing the

ratio/intensity of the OS beam in the two polarization directions. Some typical modulation curves of polarization degree "ρ" is given in Fig. 6, corresponding to different combinations of OS shifts in the two polarization directions (which can be controlled through the polarization of the OS beam). Thus, the polarization state of polaritons can be modulated flexibly using the proposed all-optical method. Here it is worth mentioning that our modulator is all-optical, and we are controlling it via an external polarized Stark beam. In this way, the waveguide effect is erasable and polarization sensitive. While the main limitations of this method is that the beam pattern of the optical Stark beam needs to be controlled to form an exact shape of the waveguide region in the cavity[36].

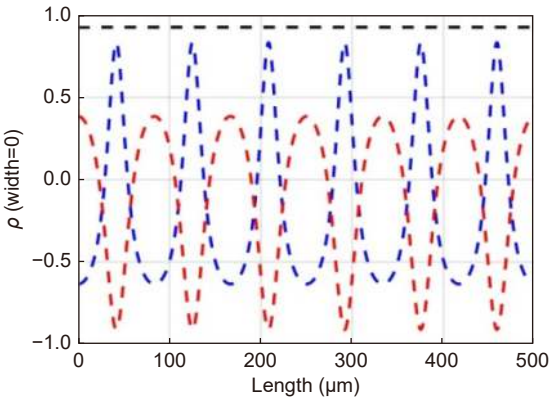

Fig. 6 | Typical modulation curves of ρ along the waveguide (x direction) for y = 0. The black curve corresponds to $\Delta E_x^{\sigma^+}$ = 5 meV and $\Delta E_x^{\sigma^-}$ = 0 meV, the blue curve corresponds to $\Delta E_x^{\sigma^+}$ = 22 meV and $\Delta E_x^{\sigma^-}$ = 5 meV, the red curve corresponds to $\Delta E_x^{\sigma^+}$ = 5 meV and $\Delta E_x^{\sigma^-}$ = 22 meV.

Conclusions

In conclusion, we have proposed an all-optical method to modulate the polarization of polaritons in a WS_2 microcavity. Spin-selective optical Stark effect has been used as a controlling and tuning parameter to modulate the output polarization and to guide the mode of polariton wavepacket. Through different combinations of OS shifts in the two spin states (i.e., control polarization degree of the OS beam), polaritonic waveguide effect with controllable birefringence can be introduced, and field distribution and polarization modulation curves of polaritons can be designed. The ultrafast response of OS effect combining with the half-matter half-light property of polariton favors the proposed structure an encouraging platform to study the basic property of quantum many body systems as well as to manipulate photons and excitons inside the TMDs materials. This work has some perspective in valleytronics and spintronics as well. As we are controlling the excitons via spin-sensitive Stark beam, so the spin-sensitive excitons-polaritons have been generated in WS_2. WS_2 has two spin-selective valleys, so we can manipulate our exciton-polaritons in both valleys via a polarized Stark beam. All these can pave the way for the study of polaritonic control and transport in TMDs microcavities, which can be helpful to the optoelectronic industry for routing and integration of polaritons for quantum information

References

1. Komineas S, Shipman SP, Venakides S. Lossless polariton solitons. *Phys D Nonlinear Phenom* **316**, 43–56 (2016).
2. Aiqin Hu, Shuai Liu, Jingyi Zhao et al. Controlling plasmon-exciton interactions through photothermal reshaping. *Opto-Electron Adv* **3**, 190017 (2020).
3. Sanvitto D, Kéna-Cohen S. The road towards polaritonic devices. *Nat Mater* **15**, 1061–1073 (2016).
4. Cancellieri E, Hayat A, Steinberg A , Giacobino E, Bramati A. Ultrafast stark-induced polaritonic switches. *Phys Rev Lett* **112**, 053601 (2014).
5. Liu XZ, Galfsky T, Sun Z, Xia FN, Lin EC et al. Strong light-matter coupling in two-dimensional atomic crystals. *Nat Photonics* **9**, 30–34 (2015).
6. Echtermeyer TJ, Milana S, Sassi U, Eiden A, Wu M et al. Surface plasmon polariton graphene Photodetectors. *Nano Lett* **16**, 8–20 (2016).
7. Zhang WL, Li XJ, Wang SS, Zheng CY, Li XF et al. Polaritonic manipulation based on the spin-selective optical Stark effect in the WS_2 and Tamm plasmon hybrid structure. *Nanoscale* **11**, 4571–4577 (2019).
8. Deng H, Haug H, Yamamoto Y. Exciton-polariton bose-einstein condensation. *Rev Mod Phys* **82**, 1489–1537 (2010).
9. Wen XM, Bi YG, Yi FS, Zhang XL, Liu YF et al. Tunable surface plasmon-polariton resonance in organic light-emitting devices based on corrugated alloy electrodes. *Opto-Electron Adv* **4**, 200024 (2021).
10. Liu FC, Zhou JD, Zhu C, Liu Z. Electric field effect in two-dimensional transition metal dichalcogenides. *Adv Funct Mater* **27**, 1602404 (2017).
11. Sie EJ, McIver JW, Lee YH, Fu L, Kong J et al. Valley-selective optical Stark effect in monolayer WS_2. *Nat Mater* **14**, 290–294 (2015).
12. LaMountain T, Bergeron H, Balla I, Stanev TK, Hersam MC et al. Valley-selective optical Stark effect probed by Kerr rotation. *Phys Rev B* **97**, 045307 (2018).
13. Bouteyre P, Nguyen HS, Lauret JS, Trippé-Allard G, Delport G et al. Room-temperature cavity polaritons with 3D hybrid perovskite: toward large-surface polaritonic devices. *ACS Photonics* **6**, 1804–1811 (2019).
14. Lerario G, Fieramosca A, Barachati F, Ballarini D, Daskalakis KS et al. Room-temperature superfluidity in a polariton condensate. *Nat Phys* **13**, 837–841 (2017).
15. Yang Y, Yang MJ, Zhu K, Johnson JC, Berry JJ et al. Stark

effect in lead iodide perovskites. *Nat Comm* **7**, 12613 (2016).
16. Zhang WL, Wu XM, Wang F, Ma R, Li XF et al. Stark effect induced microcavity polariton solitons. *Opt Express* **23**, 15762–15767 (2015).
17. Zhang WL, Rao YJ. Optical Tamm state polaritons in a quantum well microcavity with gold layers. *Chin Phys B* **21**, 057107 (2012).
18. Cuadra J, Baranov DG, Wersäll M, Verre R, Antosiewicz TJ et al. Observation of tunable charged exciton polaritons in hybrid monolayer WS_2 – plasmonic nanoantenna system. *Nano Lett* **18**, 1777–1785 (2018).
19. Klembt S, Harder TH, Egorov OA, Winkler K, Ge R et al. Exciton-polariton topological insulator. *Nature* **562**, 552–556 (2018).
20. Cancellieri G, Chiaraluce F, Gambi E, Pierleoni P. All-optical polarization modulator based on spatial soliton coupling. *J Light Technol* **14**, 513–523 (1996).
21. Novoselov KS, Mishchenko A, Carvalho A, Neto AHC. 2D materials and van der Waals heterostructures. *Science* **353**, aac9439 (2016).
22. Shahzadi M, Zhang WL, Khan MT. Exciton-polariton in WS_2 microcavity in the presence of the optical Stark effect. *Chin Opt Lett* **17**, 020014 (2019).
23. Gu J, Chakraborty B, Khatoniar M, Menon VM. A room-temperature polariton light-emitting diode based on monolayer WS_2. *Nat Nanotechnol* **14**, 1024–1028 (2019).
24. Hu T, Wang YF, Wu L, Zhang L, Shan YW et al. Strong coupling between Tamm plasmon polariton and two dimensional semiconductor excitons. *Appl Phys Lett* **110**, 051101 (2017).
25. Giovanni D, Chong WK, Dewi HA, Thirumal K, Neogi I et al. Tunable room-temperature spin-selective optical Stark effect in solution-processed layered halide perovskites. *Sci Adv* **2**, e1600477 (2016).
26. Shahzadi M, Zheng CY, Wang SS, Zhang WL. Polariton multimode interferometer controlled by optical stark shift in WS_2 microcavity. *IEEE J Quantum Electron* **56**, 9000105 (2020).
27. Voronych O, Buraczewski A, Matuszewski M, Stobińska M. Numerical modeling of exciton–polariton Bose–Einstein condensate in a microcavity. *Comput Phys Commun* **215**, 246–258 (2017).
28. Terças H, Mendonça JT. Exciton-polariton wakefields in semiconductor microcavities. *Phys Lett A* **380**, 822–827 (2016).
29. Qiu L, Chakraborty C, Dhara S, Vamivakas AN. Room-temperature valley coherence in a polaritonic system. *Nat Commun* **10**, 1513 (2019).
30. Mukherjee B, Tseng F, Gunlycke D, Amara KK, Eda G. Complex electrical permittivity of the monolayer molybdenum disulfide (MoS_2) in near UV and visible. *Opt Mater Express* **5**, 447–455 (2015).
31. Yu YL, Yu YF, Huang LJ, Peng HW, Xiong LW et al. Giant gating tunability of optical refractive index in transition metal dichalcogenide monolayers. *Nano Lett* **17**, 3613–3618 (2017).
32. Kravets VG, Wu F, Auton GH, Yu TC, Imaizumi S et al. Measurements of electrically tunable refractive index of MoS_2 monolayer and its usage in optical modulators. *npj 2D Mater Appl* **3**, 36 (2019).
33. Hichri A, Amara IB, Ayari S, Jaziri S. Exciton center-of-mass localization and dielectric environment effect in monolayer WS_2. *J Appl Phys* **121**, 235702 (2017).
34. Chakraborty B, Gu J, Sun Z, Khatoniar M, Bushati R et al. Control of strong light–matter interaction in monolayer WS_2 through electric field gating. *Nano Lett* **18**, 6455–6460 (2018).
35. Król M, Lekenta K, Mirek R, Łempicka K, Stephan D et al. Valley polarization of exciton-polaritons in monolayer WSe_2 in a tunable microcavity. *Nanoscale* **11**, 9574–9579 (2019).
36. Vella D, Ovchinnikov D, Martino N, Vega-Mayoral V, Dumcenco D et al. Unconventional electroabsorption in monolayer MoS_2. *2D Mater* **4**, 021005 (2017).

Acknowledgements

This work was supported in part by the National Natural Science Foundation of China (Grant Nos. 11974071, 61575040 and 61811530062) and in part by Sichuan Science and Technology Program (Grant No. 2018HH0148).

Competing interests

The authors declare no competing financial interests.